Rhodobacter sphaeroides Phosphoribulokinase: Binary and Ternary Complexes with Nucleotide Substrate Analogs and Effectors†

Jennifer A. Runquist,‡ Chakravarthy Narasimhan,‡ Carl E. Wolff,⊥ Hanane A. Koteiche,§,∥ and Henry M. Miziorko*,‡,∥

Department of Biochemistry, Interdisciplinary Graduate Program in Biophysics, and Biophysics Research Institute, Medical College of Wisconsin, Milwaukee, Wisconsin 53226, and Pharmacia Biotech Inc., Milwaukee, Wisconsin 53202

Received August 5, 1996; Revised Manuscript Received September 19, 1996⊗

ABSTRACT: *Rhodobacter sphaeroides* phosphoribulokinase (PRK) binds ATP substrate, as well as spectroscopically active ATP analogs (trinitrophenyl-ATP and ATPγS-acetamidoproxyl), to form stable binary complexes. Stoichiometric binding of these nucleotide triphosphates in PRK's substrate site is observed not only with wild-type enzyme but also with D42A and D169A mutants. The demonstration that these mutants contain a full complement of functional substrate binding sites indicates their substantial structural integrity and underscores the significance of their markedly diminished catalytic activity [Charlier et al. (1994) *Biochemistry 33*, 9343−9350]. Similarly, PRK forms a stable binary complex with the allosteric activator NADH. The negative allosteric effector AMP displaces activator NADH but not substrate from their respective binary complexes with enzyme. When trinitrophenyl-ATP, a fluorescent nucleotide triphosphate that functions as an alternative PRK substrate, forms a binary complex with enzyme, its fluorescence emission is enhanced and λ_{max} shifted from ∼557 to 545 nm. Upon formation of a binary PRK−NADH complex, the fluorescence emission of the dinucleotide effector is also enhanced and the λ_{max} shifted from ∼460 to 440 nm. PRK forms stable ternary complexes containing NADH and either ATP or trinitrophenyl-ATP. Due to energy transfer, NADH fluorescence in the ternary complex with trinitrophenyl-ATP is markedly quenched, allowing an estimation of the spatial separation between this novel donor/acceptor pair.

Phosphoribulokinase (PRK[1]) catalyzes the formation of ribulose 1,5-bisphosphate (RuBP), a critical step in Calvin's reductive pentose phosphate cycle. As anticipated for an enzyme responsible for a key metabolic reaction, PRK activity is regulated. Plant and algal enzymes are regulated by a thioredoxin-mediated thiol/disulfide exchange mechanism (Buchanan, 1980) that involves C16 and C55 (Porter et al., 1988). Brandes et al. (1996) have recently demonstrated that activation of the eukaryotic enzyme involves nucleophilic attack by C46 of thioredoxin *f* on C55 of PRK's disulfide. This event is followed by release of the reduced PRK when the interprotein disulfide intermediate is dissipated with concomitant formation of oxidized thioredoxin. Prokaryotic PRKs are allosterically regulated (Tabita, 1980), with NADH and AMP frequently serving as positive and negative effectors, respectively (Rindt & Ohmann, 1969; Abdelal & Schlegel, 1974).

A complete identification of amino acids within PRK's active site remains to be accomplished, but several residues have clearly been implicated on the basis of protein modification or site-directed mutagenesis studies. Protection of eukaryotic PRK's regulatory sulfhydryls from affinity labeling has been afforded by PRK substrates, suggesting an active site location for both C16 (Porter & Hartman, 1986; Krieger & Miziorko, 1986) and C55 (Porter et al., 1990). Mutagenesis work has, however, shown that neither of these residues are crucial to reaction chemistry (Milanez et al., 1991). In contrast, a specific role can be assigned to H45 and R49 of *Rhodobacter sphaeroides* PRK (Sandbaken et al., 1992); these residues markedly affect binding of the substrate ribulose 5-phosphate (Ru5P). Studies on *Chlamydomonas* PRK (Roesler et al., 1992) afford an independent confirmation of the importance of arginine for Ru5P binding to the eukaryotic enzyme. Additional studies on the *R. sphaeroides* enzyme (Charlier et al., 1994) have clearly implicated in catalysis the carboxyl groups contributed by D42 and D169. While these carboxyls have been proposed to potentially function as either active site base or activator cation ligand, a precise assignment of their function is not currently possible.

Progress in establishing the molecular events that account for RuBP synthesis would be expedited by elucidation of a PRK structure. Production of diffraction quality crystals of the *R. sphaeroides* enzyme has been reported (Roberts et al., 1995), and ongoing work (D. Harrison, unpublished observations) suggests that such structural information will become available. However, a thorough understanding of PRK's mechanisms for regulation and catalysis will require comparable information on various complexes of enzyme with substrates, products, and effectors. As a result of work

† This work was supported, in part, by Grants 93 373069181 and 96 35306 3448 to H.M.M. from USDA's National Research Initiative Competitive Research Grant Program (Photosynthesis and Respiration). H.A.K. was supported by NIH (GM-22923 to J. S. Hyde).

* Address correspondence to this author at the Department of Biochemistry. Phone: 414-456-8437. Fax: 414-266-8497.

‡ Department of Biochemistry.

§ Biophysics Research Institute.

∥ Interdisciplinary Graduate Program in Biophysics.

⊥ Pharmacia Biotech Inc.

⊗ Abstract published in *Advance ACS Abstracts,* November 1, 1996.

[1] Abbreviations: PRK, phosphoribulokinase; Ru5P, ribulose 5-phosphate; RuBP, ribulose 1,5-bisphosphate; TNP-ATP, 2′(3′)-*O*-(2,4,6-trinitrophenyl)adenosine 5′-triphosphate; ATPγSAP, adenosine 5′-*O*-[*S*-(acetamidoproxyl)-3-thiotriphosphate].

S0006-2960(96)01933-2 CCC: $12.00

aimed at supporting this objective for the *R. sphaeroides* enzyme, several stable binary and ternary model complexes have been discovered; they are identified and characterized in this report. Moreover, the potential utility of these complexes in structural studies is illustrated by a solution state investigation of the interaction between PRK-bound effector (NADH) and a nucleotide substrate. A preliminary account of portions of this report has appeared (Runquist et al., 1996).

MATERIALS AND METHODS

Materials. Adenosine 5′-monophosphoric acid, adenosine 5′-triphosphate, β-NADH, and D-ribulose 5-phosphate were purchased from Sigma Chemical Co. Sodium [^{14}C]bicarbonate, 57.38 mCi/mmol, was a product of NEN Research Products. The RuBP carboxylase required for the CO_2 fixation assay of PRK activity was isolated after expression in *Escherichia coli* JM103 using a plasmid generously provided by C. R. and S. C. Somerville. Tris and Hepes buffers were purchased from Research Organics, Inc. Chromatography media utilized for PRK isolation included reactive green-19 agarose from Sigma and Q Sepharose Fast Flow from Pharmacia Biotech. Routine protein assays employed the Bio-Rad protein assay dye reagent. For fluorescence experiments, quinine sulfate from Fisher Scientific Company and TNP-ATP [2′(3′)-*O*-(2,4,6-trinitrophenyl)adenosine 5′-triphosphate] from Molecular Probes were utilized. Adenosine 5′-*O*-[*S*-(acetamidoproxyl)-3-thiotriphosphate] (ATPγSAP) was synthesized as described by Koteiche et al. (1995).

Expression, Purification, and Assay of PRK. *E. coli* BL21-(DE3) cultures containing plasmid pETbprkwt, plasmid pETbprkD42A, or plasmid pETbprkD169A (Charlier et al., 1994) were grown at 25 °C in 1.6 L of ampicillin-containing LB media to an $OD_{600} \sim 0.7$. Expression of PRK was induced by addition of IPTG to a final concentration of 1 mM followed by 3−4 h of additional growth. The cells were collected by low-speed centrifugation and cell pellets were suspended and disrupted using a French pressure cell. A 100000*g* supernatant was prepared and subjected to Q-Sepharose anion exchange chromatography followed by affinity chromatography (Gibson & Tabita, 1987) on reactive green-19 agarose. A modified version of this protocol is followed when isolating PRK without tightly bound ATP (Koteiche et al., 1995). PRK is eluted from reactive green-19 agarose affinity resin with a buffer containing 25 mM Tris-HCl (pH 8.2), 10 mM β-mercaptoethanol, 1 mM EDTA, and 1 M KCl (Koteiche et al., 1995); as required, subsequent gel filtration chromatography using Superose 6 resin (Pharmacia) yields protein comparable in specific activity to standard PRK preparations.

For quantitative protein concentration estimates, an extinction coefficient of 50 303 M^{-1} cm^{-1} at 280 nm was used. This molar extinction coefficient was determined from amino acid composition analysis of PRK. Protein was frequently measured by the dye-binding method of Bradford (1976) using bovine serum albumin as a standard. Such protein concentration estimates are ∼1.6 times higher than the actual concentration, as determined using the molar extinction coefficient of PRK at 280 nm. Thus, dye-binding protein estimates, as well as any binding stoichiometries based on such estimates (Koteiche et al., 1995), must be accordingly corrected.

Kinetic characterization of PRK employed a radioisotopic assay that involves trapping the PRK reaction product RuBP via the RuBP carboxylase-dependent incorporation of $^{14}CO_2$ to form acid-stable [^{14}C]-3-phosphoglycerate (Paulsen & Lane, 1966). In standard assays, the final concentrations of reaction mixture components were 100 mM Hepes, pH 8.0, 1 mM DTT, 20 mM $MgCl_2$, 20 mM $KH^{14}CO_3$ (1000 dpm/nmol), 5 mM ATP, 1 mM Ru5P, 1 mM NADH, and 100 munits of recombinant RuBP carboxylase. Enzyme assays were conducted at 30 °C. Kinetic data were fit by a nonlinear regression analysis algorithm (Marquardt, 1963).

ATP Binding Measurements. Solutions (0.2 mL) containing 25 mM Tris-HCl, pH 8.0, 1 mM $MgCl_2$, PRK, and varying concentrations of ATP were prepared and incubated for 0.5 h at room temperature. In order to remove excess ATP, the incubation mix was subjected to centrifugal gel filtration (Penefsky, 1977) using Sephadex G-50 which had been pre-equilibrated with 25 mM Tris, pH 8.0. The recovered material containing the binary PRK−ATP complex was diluted to 0.25 mL for UV−vis absorption spectroscopy. The amount of ATP bound to PRK was determined by comparing the empirically determined 260/280 nm ratio with a standard curve that had been developed by plotting this absorbance ratio versus stoichiometries of known ATP/PRK mixtures.

TNP-ATP Binding Measurements. TNP-ATP binding to PRK was followed by fluorescence measurements utilizing a SLM 4800C spectrofluorometer. All spectra were corrected, as needed, for wavelength-dependent instrument response. Tris-HCl buffer (10−25 mM, pH 8.0, as indicated) was used in all experiments. For TNP-ATP titrations, the excitation wavelength was 408 nm and the emission spectra were scanned from 500 to 600 nm. In control experiments, emission spectra of PRK and Tris buffer were scanned from 500 to 600 nm and any minor contribution was subtracted from the TNP-ATP emission spectra before analysis. During titrations, sequential additions of TNP-ATP were made such that the final volume of the sample was not increased significantly (≤3%). For data analysis, values measured at the fluorescence emission peak of 545 nm for PRK-bound TNP-ATP were utilized. In addition, data reported for PRK-bound TNP-ATP were corrected for fluorescence of an equivalent amount of free TNP-ATP in Tris buffer; thus, the enhancement of fluorescence is displayed and used in all binding analyses.

NADH Binding and Displacement Measurements. NADH binding to PRK was also measured using fluorescence methods. Emission spectra were scanned from 400 to 550 nm, using 340 nm excitation. For data analysis, the increase in fluorescence at 440 nm (the emission maximum for PRK-bound NADH) was plotted after the fluorescence for an equivalent concentration of free NADH in Tris buffer had been subtracted. Thus, the enhancement of NADH fluorescence is shown in all NADH binding experiments. NADH loads onto PRK with ∼1:1 stoichiometry upon mixing the enzyme with 1−2 mM NADH. The binary PRK−NADH complex was isolated from unbound metabolite by centrifugal gel filtration using Sephadex G-50 (Penefsky, 1977); controls verified that free NADH did not elute from the column under these conditions. The concentrations of bound NADH and PRK were determined by UV−vis absorption spectropho-

tometry. This method of preparing the PRK−NADH binary complex was also utilized for NADH displacement experiments. In the AMP titration experiment, a 0.2 mL solution of 25 mM Tris buffer, pH 8.0, 1 mM NADH, and 62 μM PRK was incubated for 0.5 h at room temperature prior to removal of unbound NADH by centrifugal gel filtration. The sample was appropriately diluted for fluorescence measurements, and titration was performed by addition of small aliquots from a stock solution of AMP. The measured decrease in NADH fluorescence enhancement at 440 nm was corrected for any contribution calculated for free NADH produced by AMP displacement.

Analyses of Nonequilibrium Complex Formation. The binding stoichiometry (Davenport, 1971; Bagshaw & Harris, 1988; Kurz et al., 1992) of mono- and dinucleotides to PRK was determined from the intersection point of lines fit to the low-occupancy and plateau regions of the titration data by linear regression analyses (Grafit, v.3.0; Leatherbarrow, 1992). Calculated stoichiometries reflect binding sites per 32 kDa PRK subunit; native PRK is an octamer of 32 kDa subunits.

Energy Transfer Measurements. The efficiency of energy transfer from NADH (energy donor) to TNP-ATP (energy acceptor) was followed by donor quenching (Wu & Brand, 1994). The observed transfer efficiency (E_{obs}) was calculated from the ratio of the donor fluorescence in the presence and absence of the acceptor:

$$E_{obs} = 1 - (F_{DA}/F_D) \quad (1)$$

where F_{DA} is the fluorescence of the double-labeled sample and F_D is the fluorescence of the donor. Spectra were normalized to the same donor (NADH) concentration. For preparation of the ternary PRK−NADH−TNP-ATP complex, PRK in a 0.2 mL volume of 25 mM Tris buffer, pH 8.0, was incubated with 2 mM NADH and 0.3 mM TNP-ATP for 0.5 h at room temperature. The ternary enzyme complexes were resolved from unbound metabolites by centrifugal gel filtration (Sephadex G-50). Controls showed that neither free TNP-ATP nor NADH eluted from the G-50 column under these conditions. Concentrations of TNP-ATP, NADH, and PRK were determined by sequential subtraction. The TNP-ATP concentration was determined on the basis of A_{412} and the molar extinction coefficient (26×10^3 M^{-1} cm^{-1}). Upon subtraction of the TNP-ATP spectral contribution from the composite spectrum, the NADH concentration was determined from the absorbance at 340 nm. Upon subtraction of the NADH spectral contribution, the PRK protein concentration was determined by utilizing the molar absorption coefficient (at 280 nm) for PRK. The ternary complex generally exhibited ~1:1:1 stoichiometry. For the transfer efficiency measurement, the binary PRK−NADH complex and the ternary PRK−NADH−TNP-ATP complex were matched in NADH concentrations. The energy transfer efficiency for PRK was also determined from a titration of PRK−NADH with sequential additions of TNP-ATP to the fluorescence cuvette.

For calculation of R_0, the Forster critical distance at which the transfer efficiency is 50%, the following equation was utilized,

$$R_0 = (9.79 \times 10^3)(\kappa^2 \eta^{-4} \Phi_D J_{DA})^{1/6} \text{ (Å)} \quad (2)$$

where κ^2 is the orientation factor between donor and acceptor, η is the refractive index of the medium, Φ_D (NADH) is the quantum yield of the donor in the absence of the acceptor, and J_{DA} is the spectral overlap integral. The index of refraction, η, is 1.4 for the aqueous solution. A value of $^2/_3$, the dynamic average, was assumed for κ^2 in the calculation of R_0. This assumption seemed reasonable (Haas et al., 1978; Cerione et al., 1983) since fluorescence polarization measurements ($P = 0.34$) suggested that NADH is not bound to PRK in a totally rigid fashion.

The relative quantum yield (Φ_{NADH}) for NADH was determined by comparison to that of quinine sulfate (Φ_{QS}) (Parker & Reese, 1966), which has a quantum yield of 0.55 in 1 N H_2SO_4 (Wu & Brand, 1994). The following equation was used to calculate the quantum yield of NADH:

$$\Phi_{NADH} = F_{NADH}/F_{QS} \times OD_{QS}/OD_{NADH} \times \Phi_{QS} \quad (3)$$

The fluorescence (F) of both NADH and QS was evaluated at 450 nm after the appropriate backgrounds had been subtracted. The optical densities were measured at 340 nm.

Determination of the overlap integral between the donor and the acceptor, J_{DA}, employed the equation:

$$J_{DA} = \frac{\int_0^\infty [\{F_D(\bar{v})\epsilon_A(\bar{v})\}\bar{v}^{-4}]\, d\bar{v}}{\int_0^\infty \{F_D(\bar{v})\}\, d\bar{v}} \quad (4)$$

where F_D is the peak-normalized fluorescence spectrum of the donor, ϵ_A is the molar absorption coefficient of the acceptor, and the wave number $\bar{v}$ equals $1/\lambda$. The binary complexes PRK−NADH and PRK−TNP-ATP used for the overlap integral determination were individually produced and isolated by centrifugal gel filtration (Sephadex G-50). For the donor (NADH) emission spectrum, excitation occurred at 340 nm and emission was collected between 350 and 650 nm. For the acceptor (TNP-ATP) excitation spectrum, emission was monitored at 550 nm and data were collected upon excitation between 350 and 540 nm. After any minor contribution due to the PRK buffer spectrum was subtracted, the overlap integral was calculated by Simpson's rule for integral approximation. The calculated value for J_{DA} was used in eq 2, along with the measured quantum yield, Φ_{NADH}, to determine R_o. Due to the stoichiometric nature of ligand binding in the PRK complexes, the corrected energy transfer efficiency E_c is equivalent to the observed energy transfer efficiency E_{obs}. The average distance, r, between donor and acceptor is calculated from the Forster equation:

$$r = R_0(1/E_c - 1)^{1/6} \text{ (Å)} \quad (5)$$

RESULTS

Formation of a Binary PRK−ATP Complex. Previously, we indicated that exposure of PRK to excess ATP during elution from an affinity matrix produced enzyme that retained stoichiometric levels of ATP, even after prolonged dialysis (Koteiche et al., 1995). Samples containing fixed levels of enzyme isolated by a protocol that avoids exposure to ATP can be subsequently titrated with increasing levels of this substrate. A plot of PRK-bound nucleotide, measured after centrifugal gel filtration of these samples, displays a curve shape (Figure 1) that suggests nonequilibrium binding of nucleotide to form a stable PRK−ATP complex. Theoretical

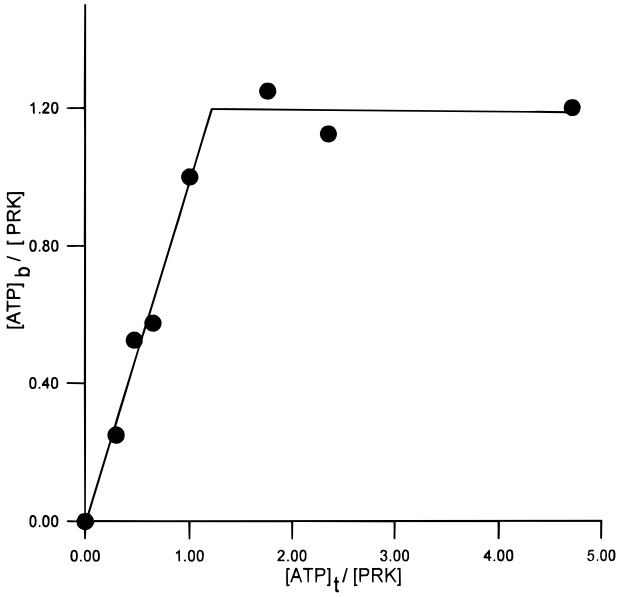

FIGURE 1: ATP titration of PRK. ATP at concentrations of 0, 5, 8, 11, 17, 30, 40, or 80 μM was added to separate 0.2 mL incubation mixes containing 1 mM $MgCl_2$, 25 mM Tris, pH 8.0, and 17 μM PRK. After removing unbound ATP by G-50 centrifugal gel filtration, the 260/280 nm ratio was measured for each sample and compared with a standard curve to establish the ATP/PRK stoichiometry, as described in Materials and Methods. This ATP/PRK stoichiometry is plotted on the ordinate versus the ratio of ATP added to the incubation mix containing 17 μM PRK. Solid lines represent linear regression fits of low- and high-occupancy data points (cf. Materials and Methods). The stoichiometry of ATP binding (1.2) was determined from the intersecting point of the two lines.

lines fit to the data in the low-occupancy and plateau regions (Davenport, 1971; Bagshaw & Harris, 1988) produce an intersection point that suggests a binding stoichiometry[2] of 1.2 ATP/site, in reasonable agreement with values measured by UV absorbance or enzymatic ATP assay after prolonged dialysis of enzyme isolated using an ATP/affinity elution protocol.

Formation of Stable Binary Complexes of PRK and Spectroscopically Active Nucleotide Substrate Analogs. TNP-ATP binding to PRK was studied by UV−vis as well as fluorescence spectroscopy. When the probe binds to PRK, its absorption maxima shifts from 408 to 412 nm, a change clearly seen when the spectrum of free nucleotide is subtracted from the spectrum of PRK-bound probe. The observed red shift implicates a hydrophobic environment for TNP-ATP in PRK (Freifelder, 1976). Such an environment is also suggested by fluorescence experiments. Buffered solutions of TNP-ATP exhibit a fluorescence emission maximum of 557 nm. When the probe binds to PRK, the emission peak shifts to 545 nm and the fluorescence is enhanced by about 6-fold. Figure 2A shows a plot of the fluorescence enhancement measured when a sample containing 5.1 μM PRK sites is titrated with increasing concentrations of TNP-ATP. Straight lines fit to the low-occupancy and plateau regions intersect at a point coincident with a probe/enzyme site ratio of 0.84, suggesting that nonequilibrium binding to form a stable PRK−TNP-ATP complex occurs. TNP-ATP binds specifically to the ATP site in PRK.

[2] Binding stoichiometries are calculated on the basis of a 32 kDa PRK subunit.

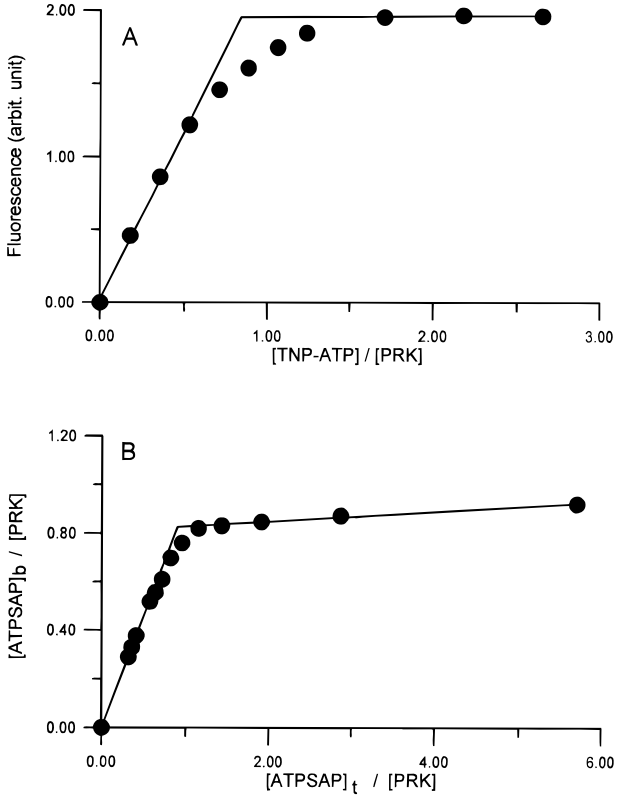

FIGURE 2: (A) Fluorescence titration of PRK with TNP-ATP. Fluorescence measurements were performed as described in Materials and Methods. Sequential additions of TNP-ATP were made to a fluorescence cuvette containing 5.1 μM PRK in 10 mM Tris, pH 8.0, from a stock solution of 0.3 mM TNP-ATP for lower occupancy and 0.8 mM for higher occupancy data points. The relative fluorescence enhancement (the total fluorescence minus that due to TNP-ATP nucleotide alone, as well as any contribution from PRK in 10 mM Tris buffer) is plotted versus the ratio of TNP-ATP added to 5.1 μM PRK present in the cuvette. (B) ESR titration of PRK with ATPγSAP. The data (Koteiche et al., 1995) presented are recalculated based on the protein concentration determined from absorbance at 280 nm and a molar extinction coefficient of 50 303 M^{-1} cm^{-1}. Varying concentrations of ATP-free PRK (3.75−67.5 μM) were added to 21 μM ATPγSAP. Binding stoichiometries for TNP-ATP (0.84) and ATPγSAP (0.83) were determined from analyses explained in the legend for Figure 1.

This is not entirely surprising, since this fluorescent analog is also an alternative PRK substrate. Using the $^{14}CO_2$ fixation assay and working at low concentrations (50−200 μM), TNP-ATP turns over at a rate comparable to that measured using similar concentrations of the physiological substrate ATP. At higher concentrations of TNP-ATP, significant substrate inhibition is observed. Addition of ATP, the authentic physiological substrate, to a preformed PRK−TNP-ATP complex results in displacement of the bound probe. The $K_{1/2}$ for probe displacement by ATP is 50 μM, which suggests that probe binding is somewhat tighter than ATP binding, an observation reported for TNP-ATP binding to several other proteins (Arora et al., 1990; Grubmeyer & Penefsky, 1981).

It is interesting to compare the binding of TNP-ATP to PRK not only with the binding of the native substrate ATP but also with that of the spin-labeled substrate analog ATPγSAP (Koteiche et al., 1995). When ATP-free PRK is titrated with ATPγSAP, a plot of the binding data also suggests nonequilibrium interaction to form a binary complex. When protein concentrations calculated on the basis of amino acid composition data are used to determine binding

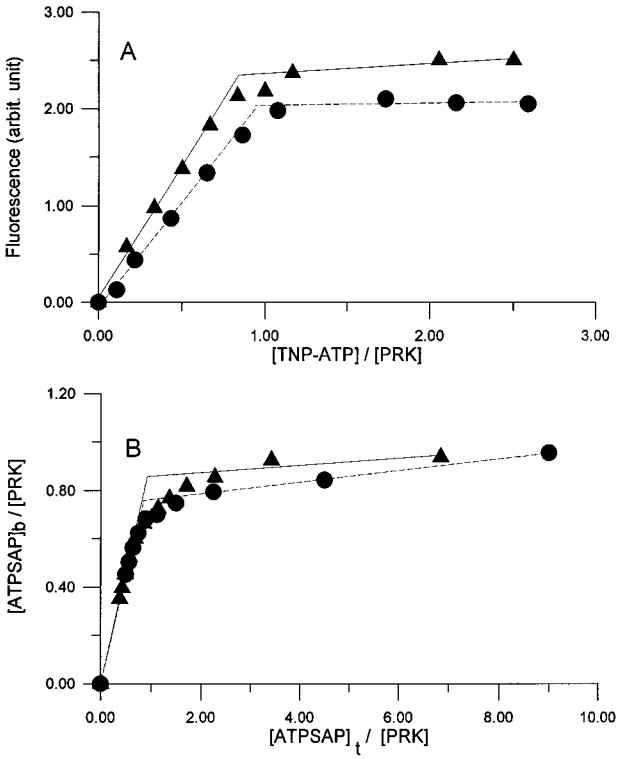

FIGURE 3: (A) Fluorescence titrations of mutant PRKs D42A and D169A with TNP-ATP. Sequential additions of TNP-ATP were made to a fluorescence cuvette containing either 5.4 μM D42A (▲) or 5.1 μM D169A (●) in 10 mM Tris, pH 8.0. The relative fluorescence enhancement is plotted versus the ratio of TNP-ATP added to the PRK mutant present in the cuvette. (B) ESR titrations of mutant PRKs D42A (▲) and D169A (●). Both mutants were purified in ATP-free form using a modified protocol involving KCl elution of PRK from the affinity column. Varying concentrations of either D42A (3.5−63 μM) or D169A (2.67−48 μM) were added to 24 μM ATPγSAP. Binding stoichiometries for the fluorescent (D42A, 0.84; D169A, 0.94) and ESR (D42A, 0.86; D169A, 0.76) probes were estimated from the intersecting points of the linear regression fits to the low- and high-occupancy data points.

ratios, theoretical lines fit to the low-occupancy and plateau regions of the resulting data plot (Figure 2B) intersect at a point that suggests a stoichiometry in excellent agreement with the estimate for fluorescent nucleotide binding to PRK's ATP site. Thus, PRK can form stable binary complexes containing stoichiometric levels of various spectroscopically active reporters.

The binary complexes prove useful in testing the structural integrity of PRK variants that form the basis for postulating the involvement of D42 and D169 in catalysis (Charlier et al., 1994). Regardless of whether TNP-ATP is used in fluorescence experiments (Figure 3A) or ATPγSAP is used in ESR measurements (Figure 3B), titrations of D42A and D169A PRKs result in binding profiles comparable to those observed with wild-type enzyme (Figure 2). Moreover, the similarity in the nucleotide/site stoichiometries, measured as described above for wild-type enzyme, indicates that the mutants contain a full complement of functional substrate binding sites. The results suggest that the mutants mimic wild-type PRK in their ability to form stable binary complexes. This demonstrated structural integrity complements our earlier report of drastically diminished catalytic efficiency to suggest that D42 and D169 remain viable candidates for participation in catalysis of RuBP formation.

Formation of a Binary PRK−NADH Complex. NADH has been suggested to be a positive effector of various bacterial PRKs (Rindt & Ohmann, 1969; Abdelal & Schlegel, 1974). The kinetic data presented in Figure 4 clearly illustrate such an effect with the recombinant *R. sphaeroides* PRK A (form I). In the presence of NADH, cooperative substrate binding occurs ($S_{1/2}$=0.5 mM). Detailed kinetic analysis of the apparent hyperbolic saturation by ATP in the absence of NADH is complicated by the onset of substrate inhibition at [ATP] > 10 mM. It is, however, clear that the observed K_m for ATP (~11 mM) increases by more than 1 order of magnitude.

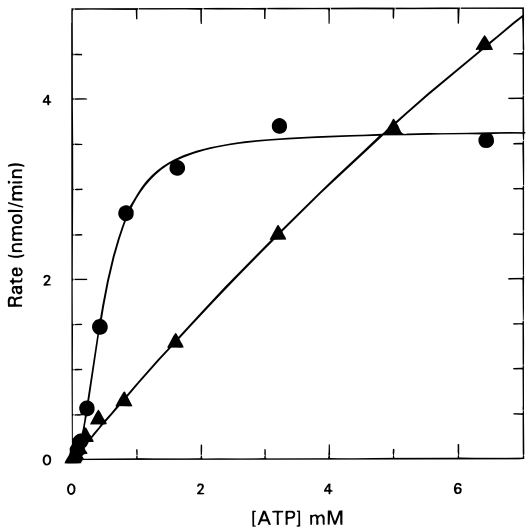

FIGURE 4: Effect of NADH on saturation of PRK by ATP. The data points are measured in the absence (▲) or presence (●) of 1 mM NADH. Either 0.6 μg of PRK (in the absence of NADH) or 0.02 μg (in the presence of NADH) was used in the CO_2 fixation assays. ATP was varied from 50 μM to 6.4 mM. Final concentrations of other assay components are specified in Materials and Methods. Enzyme activity assays were performed at 30 °C.

In order to further characterize binding of the NADH effector molecule, its interaction with PRK was followed by measuring the dinucleotide's fluorescence emission intensity at 440 nm. Figure 5A indicates that, upon interaction with PRK, NADH emission intensity is enhanced 3.8-fold and the emission λ_{max} is blue-shifted from 460 to 440 nm. Such observations suggest a relatively hydrophobic binding site for NADH. Figure 5B shows the titration of PRK (5.2 μM) with NADH. Analysis of the titration data indicates that the effector binds PRK in a nonequilibrium fashion with a stoichiometry (0.77/site; Table 1) approaching values measured for binary complexes of PRK with the nucleotide substrate or its analogs.

Allosteric stimulation of PRK activity is diminished by AMP (Rindt & Ohmann, 1969). To test whether this observation may be attributable to direct competition between the mono- and dinucleotides for a single allosteric site, the binary PRK−NADH complex was isolated by centrifugal gel filtration; stoichiometric binding of effector was verified by absorbance measurements at 340 and 280 nm. Residual enhancement of NADH fluorescence emission at 440 nm was followed after sequential additions of AMP (Figure 6). A red shift in the emission maximum of NADH to 460 nm (the λ_{max} expected for free NADH in buffer) was also observed when AMP additions exceeded stoichiometric amounts. Thus, AMP seems to quantitatively displace NADH bound to PRK. Kinetic experiments indicated that AMP inhibits NADH binding with a $K_{1/2}$ of about 200 μM,

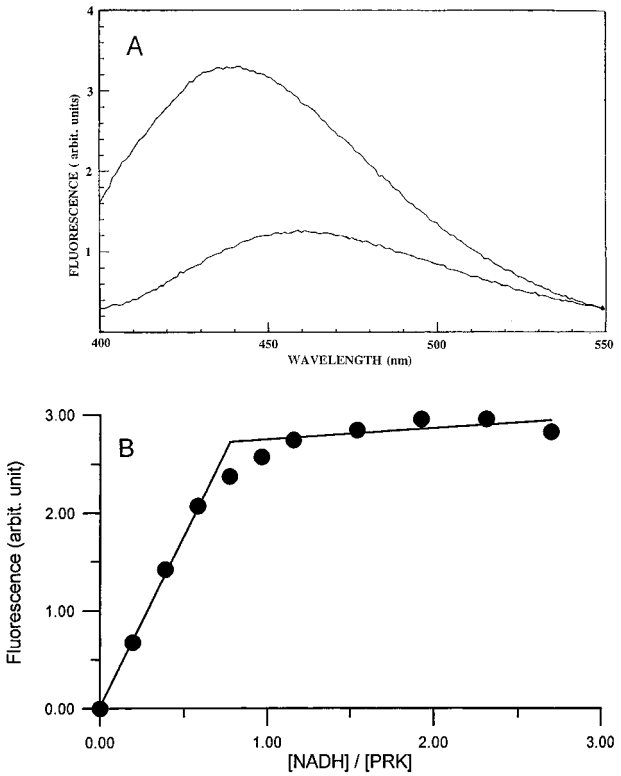

FIGURE 5: (A) Fluorescence enhancement of NADH upon binding to PRK. Fluorescence measurements were performed as described in Materials and Methods. The fluorescence emission of 4 μM NADH in the absence of PRK (lower trace) and in the presence of 6 μM PRK (upper trace) in 10 mM Tris, pH 8.0, is plotted versus wavelength. The data are corrected by substraction of any appropriate protein and buffer background contributions. In the presence of PRK, about a 3.8-fold fluorescence enhancement is observed. (B) Fluorescence titration of PRK with NADH. Sequential additions of NADH were made to a fluorescence cuvette containing 5.2 μM PRK in 10 mM Tris, pH 8. The relative fluorescence enhancement is plotted versus the ratio of NADH added to PRK present in the cuvette. The titration data were analyzed (cf. Materials and Methods) using linear regression fits (solid lines).

Table 1: Effect of AMP on Substrate Analog and Effector Binding to PRK

sample	stoichiometry −AMP	stoichiometry +AMP
PRK−NADH[a]	0.8	0
PRK−TNP-ATP[b]	1.2	1.0

[a] After isolation of the preformed binary complex PRK−NADH from an excess of ligand by centrifugal gel filtration, the concentrations of NADH and protein were determined from A_{340} and A_{280}, respectively. AMP displacement of bound NADH (Figure 6) shows that 15 μM AMP completely displaces NADH from a 5 μM sample of the binary complex. [b] After isolation of the preformed binary complex PRK−TNP-ATP from an excess of ligand by centrifugal gel filtration, concentrations of the fluorophore and protein were determined as described in Materials and Methods. Fluorescence emission of PRK-bound TNP-ATP (3.2 μM) at 545 nm was determined after AMP additions from a stock solution. Final stoichiometry tabulated above was measured in the presence of 15 μM AMP.

suggesting that under turnover conditions (in the presence of a complete set of substrates and effectors) AMP's interaction is considerably weaker than in a simpler model complex. In contrast to the effectiveness of this negative effector in displacing NADH from the *allosteric* site, AMP does not displace a nucleotide probe bound to PRK's nucleotide *substrate* site (Table 1).

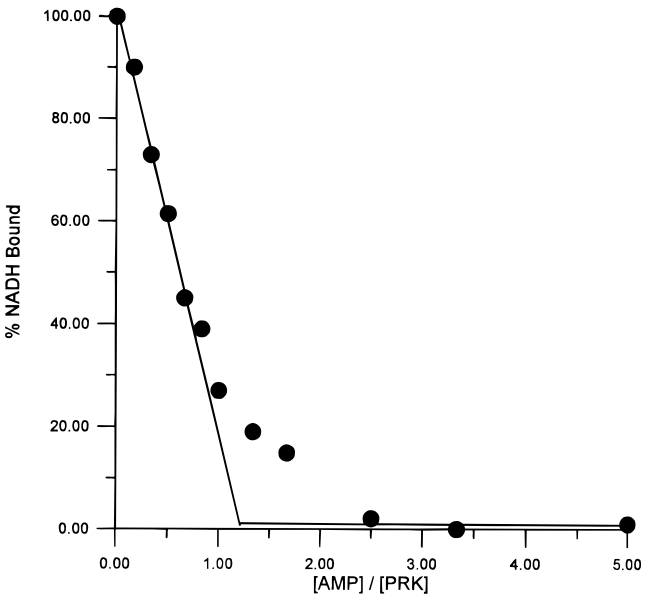

FIGURE 6: AMP displacement of NADH from the PRK−NADH binary complex. Preparation of the PRK−NADH binary complex is described in Materials and Methods. During the AMP titration, AMP was added sequentially from a stock solution to 6.0 μM PRK−NADH in 25 mM Tris, pH 8.0. The decrease in NADH fluorescence enhancement at 440 nm is plotted versus the ratio of AMP added to PRK present in the cuvette. Analysis of the titration data shows that AMP *stoichiometrically* displaces bound NADH from PRK.

Energy Transfer Measurements. As documented above, PRK forms stable binary complexes that contain stoichiometric amounts of either a fluorescent donor probe (NADH) or acceptor probe (TNP-ATP). Similarly, enzyme forms a ternary complex which is stable to isolation by centrifugal gel filtration. The ternary complex contains stoichiometric amounts of both the dinucleotide effector as well as the mononucleotide substrate analog, as estimated on the basis of extinction coefficients at 412, 340, and 280 nm for TNP-ATP, NADH, and PRK, respectively.

Fluorescence energy transfer was investigated by the donor fluorescence-quenching method (Wu & Brand, 1994). Initial work on isolated samples of stable ternary complex (PRK−NADH−TNP-ATP) suggested that the intensity of the NADH emission spectrum is diminished by about 70% and the emission λ_{max} is red-shifted from 440 to about 450 nm. In more detailed studies involving sequential addition of the acceptor TNP-ATP to the isolated binary PRK−NADH complex, a gradual quenching of the donor emission was observed accompanied by the red shift in NADH's emission λ_{max} to about 450 nm (Figure 7). That this red shift in λ_{max} and the concomitant decrease in fluorescence intensity are not simply due to displacement of PRK-bound NADH by TNP-ATP is suggested by the isolation of a stable PRK−NADH−TNP-ATP ternary complex. Additionally, a stable ternary complex can be formed and isolated using ATP instead of TNP-ATP; a similar red shift in the emission maximum of bound NADH is observed. When the non-fluorescent ATP is used to form the ternary complex, the fluorescence intensity of the bound NADH is *not* altered significantly. Thus, the observed decrease in the emission intensity of NADH may be attributed to energy transfer from NADH to TNP-ATP.

The following experiment was performed to ascertain whether the observed energy transfer is an intra- or inter-

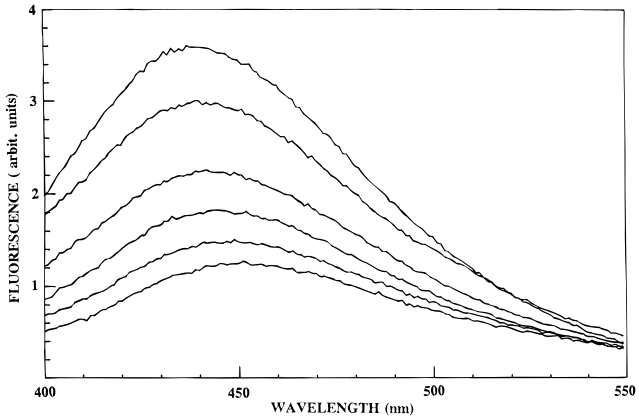

FIGURE 7: Reduction of NADH fluorescence enhancement by TNP-ATP. The PRK−NADH binary complex (6.15 μM) in 25 mM Tris, pH 8.0, was mixed with 1, 2, 3, 5, or 7 μM TNP-ATP. After each addition of the fluorescent mononucleotide, the NADH fluorescence emission was scanned from 400 to 550 nm. Data are corrected for any background spectral contribution due to PRK in the buffer. From the reduction in fluorescence attributable to bound NADH, a transfer efficiency of ~70% was calculated.

Table 2: Energy Transfer Parameters

parameter	value
emission λ_{max}, PRK−NADH	440 nm
PRK−TNP-ATP	545 nm
Φ_{NADH}	0.024
J_{DA} x 10^{14} (M^{-1} cm^3)	7.2
R_0, $\kappa^2 = {}^2/_3$ (Å)	25.2
E_c	0.70
r (Å)	21.0

molecular process. Equimolar concentrations of the isolated binary complexes PRK−NADH and PRK−TNP-ATP were admixed in a cuvette, and the fluorescence emission of NADH was measured. Neither a red shift in the emission maximum of NADH nor a significant quenching of NADH fluorescence was observed (data not shown); the measured emission intensity matched closely that of PRK−NADH alone. This suggested that the observed energy transfer is an *intramolecular* process.

From the donor-quenching data, a corrected transfer efficiency (E_c) of 0.70 was determined. The values of the spectral overlap integral, J_{DA}, and the quantum yield of NADH (Φ_D) are summarized in Table 2. Using eq 2, an R_0 of 25.3 Å was calculated for the NADH/TNP-ATP pair. Using the values of E_c and R_0 in eq 5, the distance between the donor and acceptor sites on PRK was estimated as ~21 Å. Whether this distance reflects the proximity of two sites within a single subunit or located on adjacent subunits of the octameric enzyme remains to be resolved in future experiments.

DISCUSSION

The development of methodology for facile expression and isolation of substantial quantities of *R. sphaeroides* PRK made this protein an attractive model for detailed physicochemical studies. This judgement was validated when these factors facilitated both crystallization of the enzyme as well as identification and functional assignment of several active site residues. While the prokaryotic enzyme appears to be a useful model since demonstrated structure−function relationships accounting for catalysis are easily extrapolated to the eukaryotic protein, there are some interesting differences between these PRKs. In its nonequilibrium binding of metabolites, the prokaryotic enzyme appears to differ from plant PRK. For example, while spinach PRK is commonly isolated by ATP-dependent elution from an affinity matrix, this enzyme is readily freed of bound nucleotide, rendering it quite sensitive to affinity labeling by reactive ATP analogs (Krieger & Miziorko, 1986; Miziorko et al., 1990). We have observed significant resistance of the prokaryotic enzyme to such reactive analogs that now seems attributable to its retention of a protective nucleotide. Thus, targeting of regions for directed mutagenesis of *R. sphaeroides* PRK was partially based on mapping in this protein those residues that are homologous to the amino acids identified by affinity labeling of the spinach enzyme.

In this report, we identify PRK complexes useful for solution state studies (e.g., fluorescence, ESR). In *competition* experiments, a direct and convincing demonstration of AMP displacement of NADH from the effector site has been accomplished; such interaction had only been indirectly implicated on the basis of earlier kinetic work (Rindt & Ohmann, 1969; Abdelal & Schlegel, 1974). The model complexes also allow sensitive detection of protein *conformational changes* that occur upon occupancy of substrate or effector sites. For example, the 450 nm emission maximum of NADH in the ternary PRK−ATP−NADH complex (in comparison with the 440 nm λ_{max} for the effector in the binary PRK−NADH complex) reflects a change in NADH environment when ATP binds. These complexes are shown to be useful for detection of *interactions* between probes situated in substrate and allosteric sites. The fluorescence energy transfer experiments not only illustrate this point but also provide a clear demonstration that, despite a modest R_0 value, this novel NADH/TNP-ATP donor−acceptor pair is potentially widely useful. Thus, using these PRK complexes, any of a variety of solution state approaches can generate data that are valuable not only in an independent context but also as a cross check on future models generated by high-resolution X-ray diffraction approaches.

While the binary and ternary complexes documented in this report invite a variety of additional studies, they have already been useful in confirming earlier functional assignments for two active site amino acids. Mutations at D42 and D169 have been shown to profoundly diminish PRK's catalytic efficiency (Charlier et al., 1994). The significance of these observations presumes that the mutants are not seriously structurally perturbed. Our earlier demonstration that D42 and D169 mutants retained sensitivity to allosteric activation provided some indication that they retained elements of normal function, arguing for their structural integrity. However, a stringent test of the utility of these mutants as experimental models required the identification and utilization of tools such as the spectroscopically active nucleotides used to form the model complexes. The evidence that D42 and D169 mutants contain functional substrate binding sites justifies expanded use of these proteins.

Assignment of function to key amino acids that participate in different steps of the reaction pathway will require development of a quaternary complex that includes Ru5P or an analog of this substrate. Since both ATP and TNP-ATP may be expected to turn over in any complete enzyme−substrates complex, identification of a nonreactive Ru5P analog might be viewed as a high-priority endeavor. In view

of the demonstrated structural integrity of D42 and D169 variants, a reasonable alternative approach might employ these catalytic mutants to form a quaternary complex with authentic substrates. Turnover in such a sample should occur at a rate sufficiently diminished to allow a variety of spectroscopic measurements before significant catalysis occurs.

ACKNOWLEDGMENT

The authors thank Henry Charlier for generating preliminary observations that suggested the formation of a stable PRK−ATP complex. We also thank Prof. Richard McCarty (Johns Hopkins University) for his thoughtful and timely suggestions concerning the fluorescence energy transfer experiment. Amino acid determinations were performed under the supervision of Dr. Liane Mende-Mueller at the Medical College of Wisconsin's Protein & Nucleic Acid Facility. ESR measurements utilized the facilities of the NIH National Biomedical ESR Center (RR-01008).

REFERENCES

Abdelal, A. T. H., & Schlegel, H. G. (1974) *Biochem. J. 139*, 481−489.

Arora, K. K., Shenbagamurthi, P., Fanciulli, M., & Pedersen, P. L. (1990) *J. Biol. Chem. 265*, 5324−5328.

Bagshaw, C. R., & Harris, D. A. (1988) in *Spectrophotometry and Spectrofluorimetry* (Harris, D. A., & Bashford, C. L., Eds.) pp 91−113, IRL Press, Washington, DC.

Bradford, M. (1976) *Anal. Biochem. 72*, 248−254.

Brandes, H. K., Larimer, F. W., & Hartman, F. C. (1996) *J. Biol. Chem. 271*, 3333−3335.

Buchanan, B. B. (1980) *Annu. Rev. Plant Physiol. 31*, 341−374.

Cerione, R. A., McCarty, R. E., & Hammes, G. G. (1983) *Biochemistry 22*, 769−776.

Charlier, H. A., Runquist, J. A., & Miziorko, H. M. (1994) *Biochemistry 33*, 9343−9350.

Davenport, D. (1971) in *Fluorescence Spectroscopy* (Pesce, A. J., Rosen, C. G., & Pasby, T. L., Eds.) pp 203−240, Marcel Dekker, New York.

Freifelder, D. (1976) *Physical Biochemistry: Applications to Biochemistry and Molecular Biology*, p 385, Freeman, San Francisco.

Gibson, J. L., & Tabita, F. R. (1987) *J. Bacteriol. 169*, 3685−3690.

Grubmeyer, C., & Penefsky, H. S. (1981) *J. Biol. Chem. 256*, 3718−3727.

Haas, E., Katchalski-Katzir, E., & Steinberg, I. Z. (1978) *Biochemistry 17*, 5064−5070.

Koteiche, H. A., Narasimhan, C., Runquist, J. A., & Miziorko, H. M. (1995) *Biochemistry 34*, 15068−15074.

Krieger, T. J., & Miziorko, H. M. (1986) *Biochemistry 25*, 3496−3501.

Kurz, L. C., Shah, S., Crane, B. R., Donald, L. J., Duckworth, H. W., & Drysdale, G. R. (1992) *Biochemistry 31*, 7899−7907.

Leatherbarrow, R. J. (1992) GraFit Version 3.0, Erithacus Software Ltd., Staines, U.K.

Marquardt, D. W. (1963) *SIAM J. Appl. Math. 2*, 431−441.

Milanez, S., Mural, R. J., & Hartman, F. C. (1991) *J. Biol. Chem. 266*, 10694−10699.

Miziorko, H. M., Brodt, C. A., & Krieger, T. J. (1990) *J. Biol. Chem. 265*, 3642−3647.

Parker, C. A., & Reese, W. T. (1966) *Analyst (London) 85*, 587−600.

Paulsen, J. M., & Lane, M. D. (1966) *Biochemistry 5*, 2350−2357.

Penefsky, H. S. (1977) *J. Biol. Chem. 252*, 2891−2899.

Porter, M. A., & Hartman, F. C. (1986) *Biochemistry 25*, 7314−7318.

Porter, M. A., Stringer, C. D., & Hartman, F. C. (1988) *J. Biol. Chem. 263*, 123−129.

Porter, M. A., Potter, M. D., & Hartman, F. C. (1990) *J. Protein Chem. 9*, 445−451.

Rindt, K. P., & Ohmann, E. (1969) *Biochem. Biophys. Res. Commun. 36*, 357−364.

Roberts, D. L., Runquist, J. A., Miziorko, H. M., & Kim, J. J. P. (1995) *Protein Sci. 4*, 2442−2443.

Roesler, K. R., Marcotte, B. L., & Ogren, W. L. (1992) *Plant Physiol. 98*, 1285−1289.

Runquist, J. A., Koteiche, H. A., & Miziorko, H. M. (1996) *Biochemistry 35*, 9295.

Sandbaken, M. G., Runquist, J. A., Barbieri, J. T., & Miziorko, H. M. (1992) *Biochemistry 31*, 3715−3719.

Tabita, F. R. (1980) *J. Bacteriol. 143*, 1275−1280.

Wu, P., & Brand, L. (1994) *Anal. Biochem. 218*, 1−13.

BI9619334